International Journal of Technology 15(4) 965-975 (2024)
Received November 2022 / Revised January 2023 / Accepted January 2023

International Journal of Technology

http://ijtech.eng.ui.ac.id

Garlic-induced Stable Black Gold Nanostructure: Optical, Morphological, Antibacterial, Antioxidant and Cytotoxic Properties

Harits Atika Ariyanta[1,3*], Hotlina Nainggolan[1], Siti Aysah Denti[1], Yega Segara M[1], Cahya Mukti Setiyanto[2], Indila Mayrosa[2], Widya Fatriasari[3,4], Yoki Yulizar[2], Tribidasari A. Ivandini[2]

[1]*Department of Pharmacy, Faculty of Health and Pharmacy, Universitas Gunadarma, Depok 16424, Indonesia*
[2]*Department of Chemistry, Faculty of Mathematics and Natural Sciences, Universitas Indonesia, Depok 16424, Indonesia.*
[3]*Research Center for Biomass and Bioproducts, National Research and Innovation Agency (BRIN), Jl Raya Bogor KM 46 Cibinong 16911, Indonesia*
[4]*Research Collaboration Center for Biomass-Based Nano Cosmetic, in Collaboration with National Research and Innovation Agency (BRIN), Samarinda 75123, Indonesia*

Abstract. We have successfully developed a direct, one-step phyto-synthesis of stable black gold nanostructure (AuNS) using garlic extract (GE). The presence of abundant S in GE has a high affinity for Au, forming strong Au-S bonds to induce the growth of anisotropic crystals on Au and continue to form an extensive network of nanowires resembling a dendrimer. The synthesized garlic-induced stable black AuNS was observed by a color change from brick-red to black through the addition of GE at various concentrations and confirmed by the UV–Vis spectrophotometer, particle size analyzer (PSA), transmission electron microscope (TEM), Fourier transform infrared (FTIR), and x-ray diffraction (XRD) spectrophotometer. In addition, the antibacterial, antioxidant, and cytotoxic properties of the black AuNS were studied. Black-AuNs showed no antibacterial activity on gram-negative bacteria (*Escherichia coli*) and two gram-positive bacteria (*Staphylococcus aureus* and *Bacillus subtilisin*) but had very high antioxidant activity (99.68% DPPH inhibition). The cytotoxic effect of black-AuNS was studied in normal cells and showed that the inhibition in both Vero and Chang cells was dose-dependent. These findings offer new opportunities to develop a "green" superstructure of black AuNS for other biomedical applications.

Keywords: Garlic; Green-Synthesis; Gold Nanoparticles; Nanodendrite; Nanowire

1. Introduction

Nanotechnology has become a very broad research topic in recent years, and it has piqued the interest of many researchers (Sofyan *et al.*, 2019). Particles with a nano-size leave a trace in daily human life and play an important role in various lines of biotechnology, such as the food industry, health industry, and others (Del Buono *et al.*, 2022; Ariyanta, Ivandini, and Yulizar, 2021b; Mo *et al.*, 2021; Bai *et al.*, 2020; Mei *et al.*, 2018; Menon *et al.*, 2017). Nanotechnology is generally associated with nanoparticle products with varying but regular shapes, sizes, and properties (Khan *et al.*, 2019). Plasmonic nanostructures such as gold (Au) and silver (Ag) have long attracted great interest in various fields of

*Corresponding author's email: harits@staff.gunadarma.ac.id, Tel.: +6285726703526
doi: 10.14716/ijtech.v15i4.6147

science and contributed to several aspects of life with newly unpredictable applications (Rosman *et al.*, 2021; Kalimuthu *et al.,* 2020). Localized surface plasmon resonance (LSPR) generates their optical properties, which are highly dependent on particle size and morphology. Gold nanostructures (AuNS) ranging in size and morphology from 0 to 3D, such as quantum dots, spheres, thin films, rods, wires, and dendrites, have been synthesized using various methods depending on the application (Khumaeni, Sutanto, and Budi, 2019).

Black AuNS is a potential super particle that has been reported to have broadband absorption properties throughout the visible and infrared domains. Their unique morphology is driven by the anisotropic growth of small nanoparticles, leading to the self-assembly of an extensive network of nanowires that resembles a dendrimer. Indeed, the unique properties of black AuNS are suitable for applications such as photothermal therapy, surface-enhanced spectroscopy, or solar energy conversion. Several successful fabrication methods of black AuNS have been reported. Aqueous black colloids of gold nanostructured were synthesized with the simple addition of $NaBH_4$ to $HAuCl_4$ at a very precise concentration in ice temperature. Unique reticular gold nanostructure produced in this approach exhibits high conductivity and low reflection. However, black colloids produced are only stable at room temperature for up to one week before forming a black precipitate (Stanca *et al.*, 2015). Similar AuNS morphology was also fabricated using X and Y-shaped DNA as templates, assisted by a stirring process for 10 hours. The findings show that LSPR properties in the near-infrared region are unique, allowing for deep-tissue penetrating photothermal therapy. Colloidal stability and cellular uptake were obtained after introducing the positively charged lipoic-acid-derived quaternary ammonium ligand and thiolated poly(ethylene glycol) (Song *et al.*, 2016). A direct one-step chemical synthesis at high temperatures has been reported to fabricate colloidal black gold superstructures through solvophobic interaction with the mixture of oleylamine and ethylene glycol as a solvent (Kwon *et al.*, 2018). One-step synthesis was also carried out by mixing gold precursor salt and sodium citrate at room temperature in a basic pH (Sarhan *et al.*, 2022). Small gold nanoparticles (AuNP) were chemically deposited on dendritic fibrous nano-silica to enhance nucleation growth (Dhiman *et al.*, 2019), also using the overcurrent electrodeposition method to produce black AuNS (Yu *et al.*, 2020). However, the preparation of the aforementioned black AuNS synthesis methods requires multiple steps involving various solvents and heat, and is time-consuming. A simple method with a green approach is a challenge for the fabrication of black AuNS. Herein, we report the fabrication of black AuNS using the induction of garlic as an organic initiator to promote anisotropic growth.

Generally, the gold nanoparticles (AuNP) green synthesis method substitutes secondary metabolites from plant extracts for strong reducing agents such as $NaBH_4$ to reduce Au^{3+} to Au^0 and produce conventional spherical particles. However, in this study, $NaBH_4$ was used as an Au^{3+} reducing agent to produce Au^0 crystal seed, and garlic extract was used to drive further anisotropic Au^0 crystal growth. Garlic (*Allium sativum L.*) is recognized for its high organosulfur (S) content, with 3% allicin being a predominant form (Gutiérrez-del-Río, Fernández, and Lombó, 2018), and its wide availability. The abundance of S in garlic extract (GE) results in a strong Au-S interaction, which facilitates the anisotropic growth of Au^0 crystals (Ariyanta, Ivandini, and Yulizar, 2021a). Through rapid adsorption between the headgroup (S) - surface (Au) interaction as well as van der Waals interaction between the alkyl chains, sulfur-containing molecules such as alkanethiols or dialkyl disulfides can form self-assembled monolayers (SAMs) on the Au surface (Xue *et al.*, 2014; Tachibana *et al.*, 2002). Therefore, S can induce anisotropic crystal growth in Au to form dendrites with many long branches so that the surface area is larger. Furthermore, in this study, garlic-induced black AuNS has excellent room temperature stability. These findings support the green-

chemistry approach, providing a simple, inexpensive, and time-efficient method. We also investigated the antibacterial, antioxidant, and cytotoxic properties of the synthesized black AuNS. To the best of our knowledge, studies on the application of black AuNS as a broadband light absorber, photothermal reaction, sensitive solar cells, or a substrate for Raman spectroscopy have been reported. However, studies on antibacterial, antioxidant, and cytotoxic properties have not been carried out, which would be required to investigate other biomedical applications.

2. Methods

2.1. Materials and Characterization

White garlic was purchased from a traditional market located in Depok, Jawa Barat, Indonesia. Tetrachloroauric(III) acid trihydrate 99% ($HAuCl_4.3H_2O$), ethanol, nutrient agar, barium chloride dihydrate ($BaCl_2.2H_2O$), sodium chloride (NaCl), sulfuric acid (H_2SO_4), 2,2-diphenyl-1-Picrylhydrazyl (DPPH), 3-(4,5-dimethylthiazol-2-yl)-2,5-diphenyl tetrazolium bromide (MTT), fetal bovine serum (FBS) and dulbecco's modified eagle medium (DMEM) were purchased from Sigma Aldrich. Vero (ATCC CCL-81) and Chang cell (ATCC CCL-13) were obtained from the Primate Anima Study Center of Bogor Agricultural Institute.

Material characterization was carried out using several analytical instruments, including an IR Prestige-21 Shimadzu Fourier Transform Infra Red (FTIR), Shimadzu 2600 UV-Vis spectrophotometer, Malvern Zetasizer Nano ZSP *Particle Size Analyzer* (PSA), Hitachi H9500 Transmission Electron Microscope (TEM), and Miniflex 600-Rigaku X-Ray Analytical Instrument X-Ray Diffraction (XRD).

2.2. Preparation of Garlic Extract

To prepare the garlic extract (GE), the salting out extraction (SOE) method was used with slight modifications based on previous studies (Ariyanta, Ivandini, and Yulizar, 2021a). Initially, 100 grams of washed and dried garlic was blended with 20 mL of water, and the resulting garlic juice was sonicated for 20 minutes with 300 mL of ethanol p.a. The resulting mixture was then filtered, and the filtrate was taken to the SOE system, which consisted of a mixture of excess ammonium sulfate and ethanol. Following the SOE process, an organic phase containing allicin was obtained, and the GE was stored in a freezer until it was used for synthesis.

2.3. Synthesis of Garlic-Induced Black-AuNS

Garlic-induced black AuNS was performed by adding 35 µL of $HAuCl_4$ 5 x 10^{-3} M to 12.5 mL of distilled water with the help of a magnetic stirrer. The resulting solution was added to 35 µL of GE with varying concentrations of 1, 5, 10, and 100% and 62µL of fresh $NaBH_4$ 0.35M to produce AuNS-1, AuNS-5, AuNS-10, and AuNS-100, respectively. The mixture was stirred for 10 minutes until a color change occurred and was further characterized using a UV-Vis spectrophotometer, FTIR, XRD, PSA, and TEM. In comparison, AuNP synthesis was carried out using the same procedure with 5% GE but without the addition of $NaBH_4$ and was carried out for 2 hours under UV lamp irradiation.

2.4. Antibacterial Activity Assay

The well diffusion method was used in this study to test the antibacterial activity of AuNS against three bacterial strains: *Staphylococcus aureus, Escherichia coli, and Bacillus subtilis*. To standardize the bacterial suspension, the McFarland turbidity standard of 0.5 was used. The NA media was sterilized and then cultured for bacteria, and a perforator no 5 was used to perforate the media to form wells. Each well was filled with 50 µL of AuNS-1, AuNS-5, AuNS-10, AuNS-100, AuNP, negative control, or positive control

(chloramphenicol). The petri dishes were incubated at 37°C for 24 hours, and the bacterial inhibition zone was observed and measured using a calliper.

2.5. DPPH Radical Scavenging Assay

The antioxidant activity of the AuNPs synthesized was determined using the DPPH free radical scavenging assay. About 2 mL of freshly prepared DPPH solution (0.004% w/v) was mixed with 100 µg/mL of AuNS using a vortex and kept in the dark at room temperature for 1 h. The absorbance of the control and treated DPPH was measured at 517 nm, and the inhibition percentage was calculated using equation 1:

$$\% I = [(A_i - A_t)/A_i] \times 100 \quad (1)$$

Where $\% I$ is the inhibition percentage, A_i is the absorbance of the control, and A_t is the absorbance of the treated DPPH.

2.6. MTT Assay

In-vitro cytotoxic analysis was done to analyze the effect of AuNS on normal cell inhibition using MTT. This method was carried out by growing Vero (ATCC CCL-81) and Chang (ATCC CCL-13) cells with a concentration of 5000 cells in 100µl DMEM supplemented with Fetal Bovine Serum (FBS) of 5%, Penicillin of 100U/mL and streptomycin 100ug/mL. The sample of AuNS with a different concentration was added after the cells were 50% confluent (24 h). On day 3, the MTT test was performed by adding 10µl MTT of 5mg/mL per well and incubating them at 37ºC for 4 h. The media was removed after incubation, and ethanol was added to dissolve the formazan crystals. The absorbance value was measured at a wavelength of 595 nm, and the inhibition percentage was calculated using equation 2:

$$\% \, Inhibition = 100 - \left(\frac{control - sample}{control}\right) \times 100 \quad (2)$$

3. Results and Discussion

3.1. Characterization of Garlic-Induced Black AuNS

The GE obtained through the SOE method was characterized using FTIR to analyze their functional groups before being used for AuNS synthesis. The GE FTIR spectra in Figure 1 shows the absorption at a wavenumber of 3000-3300, 1610, 1450, 1130, 937, and 580 cm^{-1} indicating the vibration of O-H stretching, C=C stretching, -O-H bending in carboxylic, S=O sulfoxide, γ-C–H deformation in $=CH_2$, and C-H bending in alkynes, respectively. These FTIR spectra are in agreement with our previous study showing the presence of allicin in GE (Ariyanta, Ivandini, and Yulizar, 2021a).

The synthesis of AuNS was performed by reducing Au^{3+} from $HAuCl_4$ with $NaBH_4$ to produce Au^0 crystal seed. Next, GE was added to induce anisotropic growth. Organic molecules tend to selectively bind to one face of the nanocrystal, causing it to extend asymmetrically (Stanca *et al.*, 2015). Given the high affinity of Au-S, allicin present in GE could strongly bind to the surface of the growing crystal, resulting in anisotropic growth (McCarthy *et al.*, 2018).

Figure 2a shows the UV-Vis absorbance of AuNS in different concentrations of the added GE. A sharp absorption peak at a wavelength of 520 nm occurs when 1% GE is added, which is associated with the LSPR of spherical AuNP and gradually decreases with increasing concentration due to a color change of the mixture caused by a structural change. According to the UV-Vis spectrophotometry results, adding 1% GE visually produces a brick red color, which darkens with the addition of 5% GE, then turns dark purple with the addition of 10%

GE and finally black with the addition of 100% GE. Green synthesis of AuNP without $NaBH_4$ under UV lamp irradiation was performed as a comparison. The colloid produced was pink in color and had poor stability (less than 7 days), as indicated by the formation of a black precipitate. In contrast, AuNS-100 showed very good stability until the 35th day of observation, as seen from the insignificant shift in wavelength and decrease in absorbance (Figure 2b). For 35 days, the black color obtained on AuNS-100 remained stable, with no precipitate forming. At the appropriate concentration, GE can also act as a capping agent, influencing the stability of AuNS. This can be seen in their FTIR spectra, which show the wavenumber shift of GE before and after being used for AuNS synthesis (Figure 1).

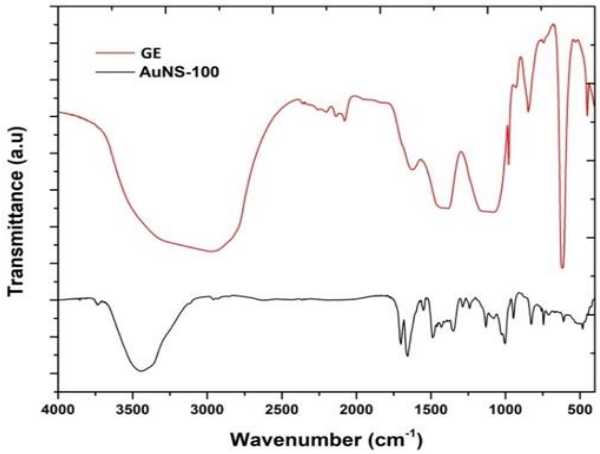

Figure 1 The FTIR spectra of (GE) and AuNS-100

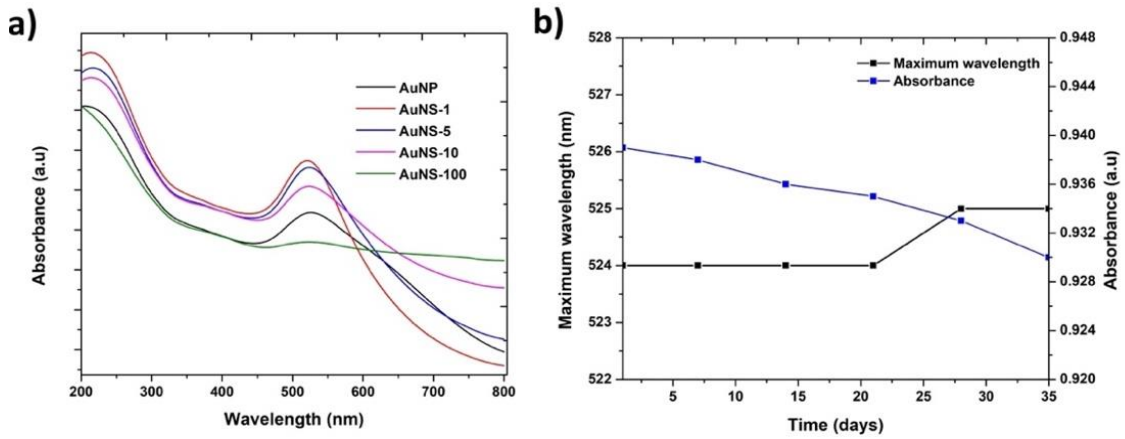

Figure 2 (a) UV-Vis absorption spectra of AuNP & various AuNS and (b) stability studies of AuNS-100

The vibration of the O-H stretching of GE shifted to 3400 cm^{-1}, the C=C stretching shifted to 1620 cm^{-1}, and S=O sulfoxide shifted to 1015 cm^{-1}. These small shifts are due to the interaction of the GE functional groups on the surface of AuNS (Yulizar *et al.*, 2017).

Furthermore, the zeta potential value of AuNS shifted to the right from -68 mV/s, -48 mV/s, -36 mV/s to -33 mV/s with the addition of 1, 5, 10, and 100 % GE, respectively (Figure 3a). Some reports mention that nanoparticles with a zeta potential close to +/- 30 mVs are considered as a stable colloidal suspension system that prevents nanoparticle aggregation (Deon Pompeu *et al.*, 2018) (Figure 3b).

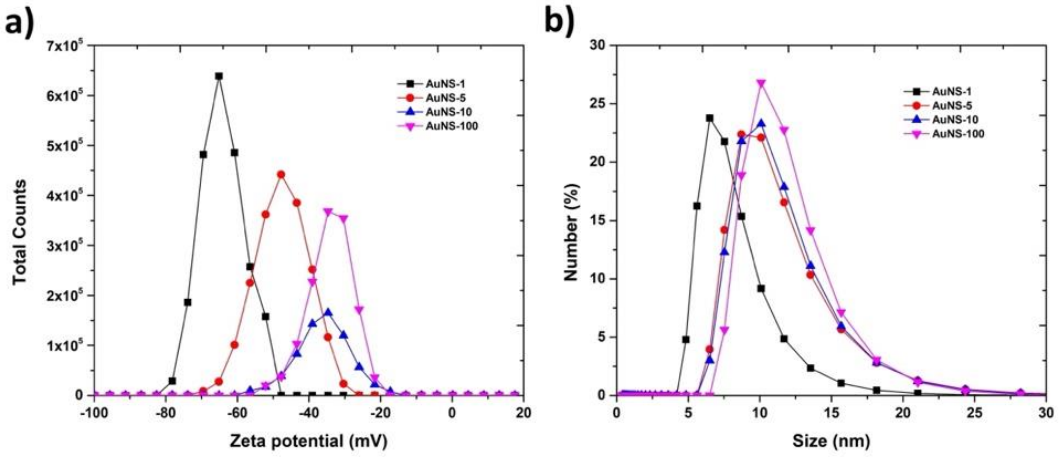

Figure 3 (a) Zeta potential and (b) Size distribution curves of various AuNS

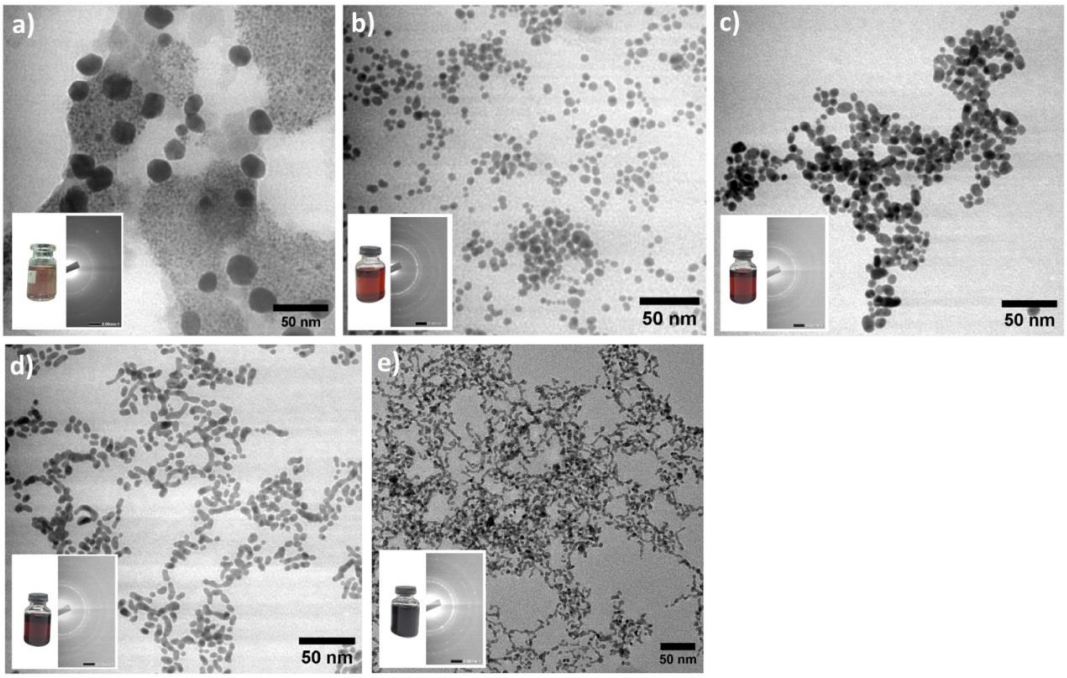

Figure 4 TEM image of (a) AuNP, (b) AuNS-1, (c) AuNS-5, (d) AuNS-10, and (e) AuNS-100

The TEM image in Figure 4 confirms the results of the previous analysis. Figure 4a depicts the morphology of AuNP synthesized without $NaBH_4$ under UV lamp irradiation. The resulting particle size appears to be larger than AuNS in diameter. The addition of 1% GE resulted in small spherical gold particles with diameters ranging from 3 to 7 nm and a red brick colloid (Figure 4b). When the GE concentration was raised to 5%, the small spherical gold particles became closer together and coalesced into a larger size of 10-15 nm (Figure 4c). This was continued until the addition of 10% GE caused spheres to assemble and fuse to form short dendrite structures (Figure 4d). Finally, Figure 4e shows the formation of an extensive network of dendrite structures at 100% GE increments.

Based on the results obtained, the growth mechanism of the synthesized garlic-induced black AuNS can be proposed. Initially, the small gold particles resulting from the reduction of Au^{3+} to Au^0 by $NaBH_4$ undergo self-assembly to form a short dendrite structure. The growth then continues due to the strong binding affinity of allicin to Au, leading to the formation of an extensive dendrimer (Figure 5). It is worth noting that when the volume of

100% GE was increased under the same synthesis conditions, a black precipitate with a clear supernatant gradually formed (data not shown).

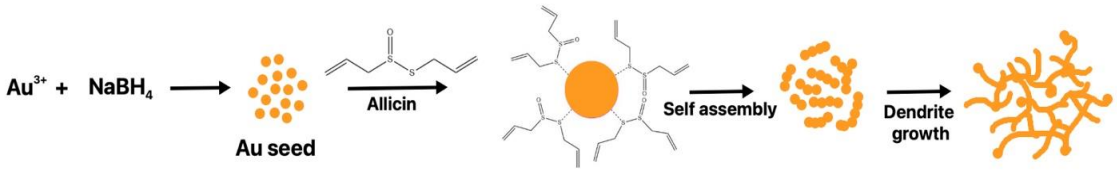

Figure 5 The proposed growth mechanism of garlic-induced black AuNS

XRD spectrometry was utilized to confirm the crystal structure of the black AuNS. XRD pattern of Figure 6 identifies peaks for face-centered cubic (fcc) polycrystalline gold at 2θ of 38.53°, 44.63°, 64.66°, and 78.75°, corresponding to (111), (200), (220) and (311) planes, which match with JCPDS Au number 04.0748. No other peaks of crystallographic impurities were found to confirm the purity of the gold crystallite.

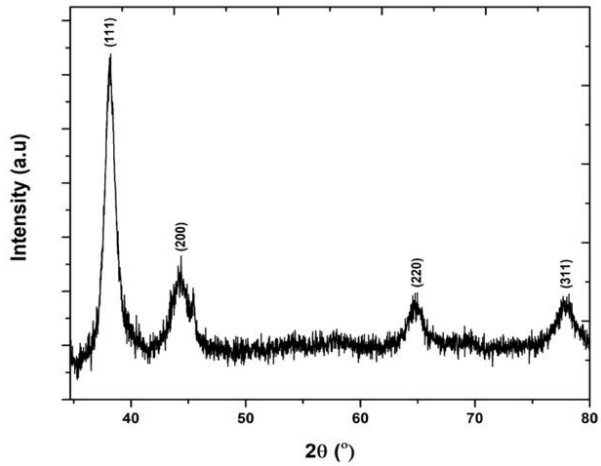

Figure 6 X-Ray diffraction spectrum of black AuNS-100

3.2. Antimicrobial Properties of Garlic-Induced Black AuNS

In this work, antimicrobial activity towards *Escherichia coli*, *Staphylococcus aureus,* and *Bacillus subtilis* showed negative results for AuNP, AuNS-1, AuNS-5, AuNS-10, dan AuNS 100. This is in accordance with previous studies that reported that AuNS did not have antibacterial activity on both gram-positive and gram-negative bacteria. The antimicrobial activity of co-existing chemicals involved during the synthesis that was not completely removed from the surface of the AuNS could explain why they appear to have antimicrobial activity (Zhang *et al.*, 2015). However, the antibacterial activity of AuNS is affected by various factors, including the method of synthesis, particle size, particle shape, surface charge, species sensitivity, and bacterial tolerance (Shahriari *et al.*, 2019). AuNS can also act as an antibiotic delivery agent or carrier that can enhance its antimicrobial effect of it (Payne *et al.*, 2016). Therefore, AuNS can be modified to have antimicrobial activity by changing its structure or adding other active substances (Su *et al.*, 2020).

3.3. Antioxidant Properties of Garlic-Induced Black AuNS

Oxidative stress is caused by an imbalance between antioxidants and free radicals, which can be harmful to human health. Antioxidant compounds play an important role in inhibiting the production and neutralizing free radicals (Parcheta *et al.*, 2021).

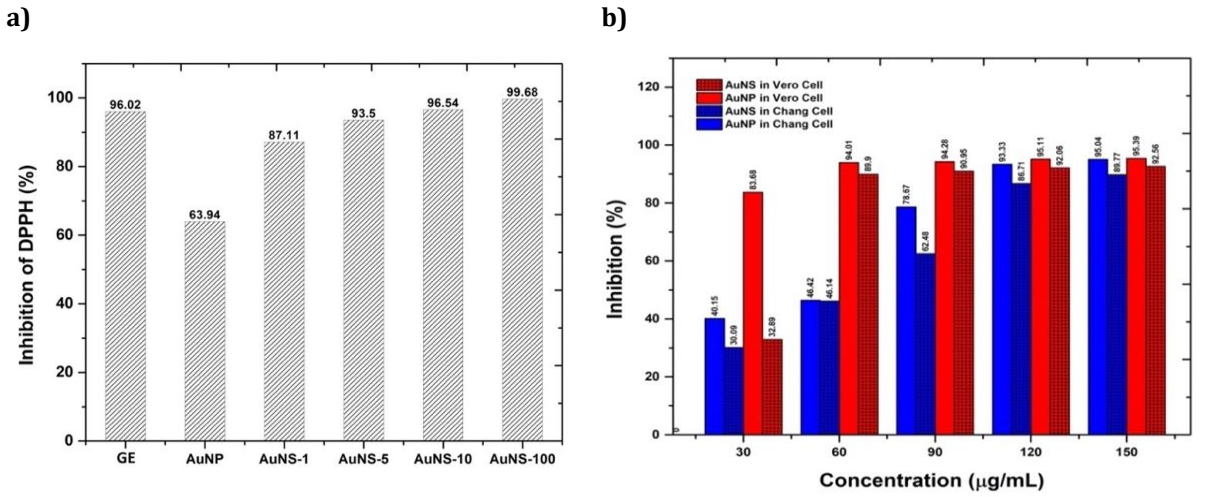

Figure 7 a) DPPH free radical scavenging activity of 100μg/mL GE, AuNP, and various AuNS towards 0.004% (w/v) DPPH solution; b) In vitro cytotoxicity of AuNP and AuNS-100 against Vero and Chang cells

The antioxidant activity of AuNS and AuNP, as shown in Figure 7a, was compared to that of GE in this study. At the same volume of particle addition to DPPH, black AuNS-100 was able to inhibit DPPH by 99.68%. Meanwhile, AuNP was only able to inhibit DPPH by 63.94%. The ability of these different antioxidants depends on the chemical composition, particle size, and surface layer of AuNPs, resulting in different physical and chemical properties, including their interactions to neutralize free radicals (Ilyas *et al.*, 2022).

3.4. Cytotoxic Properties of Garlic-Induced Black AuNS

The cytotoxic effects of AuNP are commonly evaluated using the MTT assay method on both cancerous and normal cells. Studies indicate that it has a cytotoxic effect on cells in vitro (El-Borady, Fawzy, and Hosny, 2021). The cytotoxicity of nanoparticles is affected by several factors, including size, shape, surface charge, chemistry, and surface modification (Nikzamir, Akbarzadeh, and Panahi, 2021). The biological media treatment's characteristics, preparations, and physicochemical properties can also influence nanoparticle toxicity's magnitude (Sani, Cao, and Cui, 2021).

At a concentration of 30 μg/mL, black AuNS-100 inhibited normal cells (Vero and Chang cells) with a low percentage of inhibition. The inhibition of black AuNS-100 was dose-dependent in both Vero and Chang cells. Whereas the percentage of inhibition against vero cells in AuNP was already high (83.68%) at 30 μg/mL, the percentage of inhibition against chang cells was nearly the same as in black AuNS-100 (Figure 7b).

The mechanism of AuNS in inhibiting cells is due to their ability to penetrate cells, releasing large amounts of ions that cause toxicity, and apoptosis occurs (Liu *et al.*, 2019). Furthermore, cytotoxicity reactions are influenced by molecular reactions of reactive oxygen species (ROS) as by-products in cells (Sani, Cao, and Cui, 2021). ROS binds to cellular organelles, oxidizing and reducing macromolecules (DNA, lipids, proteins), causing significant oxidative damage to cells (Bin-Jumah *et al.*, 2020).

4. Conclusions

In summary, we successfully developed a one-step “green” synthesis of black-AuNS using GE. The presence of S in GE promotes the formation of strong Au-S interaction that induces the anisotropic growth of the AuNS. Visually, there was a color change during the synthesis process from brick-red to black through the addition of GE in various

concentrations. The black color obtained on AuNS-100 has excellent stability, with morphology in the form of a dense network of branched particles mimicking dendrimers. Furthermore, the antibacterial, antioxidant, and cytotoxicity properties of black AuNS were investigated. Black-AuNS had very high antioxidant activity but no antibacterial activity against gram-negative bacteria (*Escherichia coli*) and two gram-positive bacteria (*Staphylococcus aureus* and *Bacillus subtilis*). The cytotoxic effect of black-AuNS on normal cells was also evaluated, and it was discovered that the inhibition was dose-dependent in both Vero and Chang cells. These findings open up new avenues for developing a "green" superstructure of black AuNS for other biomedical applications.

Acknowledgments

This work was funded by Hibah Penelitian Dasar Kompetitif Nasional (PDKN) 2022, No. 033/E5/PG.02.00/2022 from the Ministry of Education, Culture, Research and Technology of Indonesia through the Higher Education Service Institute of Region III (LLDIKTI III) and the Directorate of Research and Community service, Universitas Gunadarma.

References

Ariyanta, H.A., Ivandini, T.A., Yulizar, Y., 2021a. A Novel Way of the Synthesis of Three-Dimensional (3D) MoS 2 Cauliflowers Using Allicin. *Chemical Physics Letters*, Volume 767, p. 138345

Ariyanta, H.A., Ivandini, T.A., Yulizar, Y., 2021b. Poly(Methyl Orange)-Modified NiO/MoS2/SPCE for a Non-Enzymatic Detection of Cholesterol. *FlatChem*, Volume 29, p. 100285

Bin-Jumah, M.N., Al-Abdan, M., Al-Basher, G., Alarifi, S., 2020. Molecular Mechanism of Cytotoxicity, Genotoxicity, and Anticancer Potential of Green Gold Nanoparticles on Human Liver Normal and Cancerous Cells. *Dose-Response*, Volume 18(2), p. 1559325820912154

Bai, L., Jiang, F., Wang, R., Lee, C., Wang, H., Zhang, W., Jiang, W., Li, D., Ji, B., Li, Z., Gao, S., Xie, J., Ma, Q., 2020. Ultrathin Gold Nanowires to Enhance Radiation Therapy. *Journal of Nanobiotechnology*, Volume 18, p. 131

Del Buono, D., Luzi, F., Tolisano, C., Puglia, D., Di Michele, A., 2022. Synthesis of a Lignin/Zinc Oxide Hybrid Nanoparticles System and Its Application by Nano-Priming in Maize. *Nanomaterials*, Volume 12, p.568

Deon-Pompeu, L., Pinheiro-Pinton, A., Goulart-Finger, M., Gorski-Cadó, R., Severo, d.A.V., Pinheiro, L., Otavio-Bulhões, L., 2018. Evaluation of Stability of Aqueous Dispersions Using Zeta Potential Data Study. *Disciplinarum Scientia,* Volume 19(3), p. 381–388

Dhiman, M., Maity, A., Das, A., Belgamwar, R., Chalke, B., Lee, Y., Sim, K., Nam, J. M., & Polshettiwar, V., 2019. Plasmonic Colloidosomes of Black Gold for Solar Energy Harvesting and Hotspots Directed Catalysis for CO2 to Fuel Conversion. *Chemical Science*, Volume 10(27), pp. 6594–6603

El-Borady, O.M., Fawzy, M., Hosny, M., 2021. Antioxidant, Anticancer and Enhanced Photocatalytic Potentials of Gold Nanoparticles Biosynthesized by Common Reed Leaf Extract. *Applied Nanoscience*, Volume 13, pp. 3149–3160

Gutiérrez-del-Río, I., Fernández, J., Lombó, F., 2018. Plant Nutraceuticals as Antimicrobial Agents in Food Preservation: Terpenoids, Polyphenols and Thiols. *International Journal of Antimicrobial Agents*, Volume 52(3), pp. 309–315

Ilyas, M., Arif, M., Ahmad, A., Ullah, H., Adnan, F., Khan, S., Rahman, F., Khan, I., Nadeem-Khan, M., Muhammad, S., Shah, S., Khan, M.N., 2022. Biogenic Synthesis of Gold Nanoparticles, Characterization and Their Biomedical Applications. *International Journal of Biomedical Materials Research*, Volume 10(2), pp. 39–52

Kalimuthu, K., Cha, B.S., Kim, S., Park, K.S., 2020. Eco-Friendly Synthesis and Biomedical Applications of Gold Nanoparticles: A Review. *Microchemical Journal*, Volume 152, p. 104296

Khan, T., Ullah, N., Khan, M.A., Mashwani, Z.ur.R., Nadhman, A., 2019. Plant-Based Gold Nanoparticles; A Comprehensive Review of The Decade-Long Research on Synthesis, Mechanistic Aspects and Diverse Applications. *Advances in Colloid and Interface Science*, Volume 272, p. 102017

Khumaeni, A., Sutanto, H., Budi, W.S., 2019. The Role of Laser Irradiance, Pulse Repetition Rate, and Liquid Media in The Synthesis of Gold Nanoparticles by The Laser Ablation Method Using an Nd: YAG Laser 1064 nm at Low Energy. *International Journal of Technology*, Volume 10(5), pp. 961–969

Kwon, N., Oh, H., Kim, R., Sinha, A., Kim, J., Shin, J., Chon, J.W.M., Lim, B., 2018. Direct Chemical Synthesis of Plasmonic Black Colloidal Gold Superparticles with Broadband Absorption Properties. *Nano Letters*, Volume 18(9), pp. 5927–5932

Liu, R., Pei, Q., Shou, T., Zhang, W., Hu, J., Li, W., 2019. Apoptotic Effect of Green Synthesized Gold Nanoparticles from *Curcuma Wenyujin Extract* Against Human Renal Cell Carcinoma A498 Cells. *International Journal of Nanomedicine*, Volume 14, pp. 4091–4103

McCarthy, S.A., Ratkic, R., Purcell-Milton, F., Perova, T.S., Gun'ko, Y.K., 2018. Adaptable Surfactant-Mediated Method for The Preparation of Anisotropic Metal Chalcogenide Nanomaterials. *Scientific Reports*, Volume 8(1), p. 2860

Mei, X., Wei, Q., Long, H., Yu, Z., Deng, Z., Meng, L., Wang, J., Luo, J., Lin, C. T., Ma, L., Zheng, K., Hu, N, 2018. Long-Term Stability of Au Nanoparticle-Anchored Porous Boron-Doped Diamond Hybrid Electrode for Enhanced Dopamine Detection. *Electrochimica Acta*, Volume 271, pp. 84–91

Menon, S., Rajeshkumar, S., Kumar, V., 2017. A Review on Biogenic Synthesis of Gold Nanoparticles, Characterization, and its Applications. *Resource-Efficient Technologies*, Volume 3(4), pp. 516–527

Mo, D., Li, X., Chen, Y., Jiang, Y., Gan, C., Zhang, Y., Li, W., Huang, Y., Cui, J., 2021. Fabrication and Evaluation Of Slow-Release Lignin-Based Avermectin Nano-Delivery System With UV-Shielding Property. *Scientific Reports*, Volume 11, p. 23248

Nikzamir, M., Akbarzadeh, A., Panahi, Y., 2021. An Overview on Nanoparticles Used in Biomedicine and Their Cytotoxicity. *Journal of Drug Delivery Science and Technology*, Volume 61, p. 102316

Parcheta, M., Świsłocka, R., Orzechowska, S., Akimowicz, M., Choińska, R., Lewandowski, W., 2021. Recent Developments in Effective Antioxidants: The Structure and Antioxidant Properties. *Materials*, Volume 14(8), p. 14081984

Payne, J.N., Waghwani, H.K., Connor, M.G., Hamilton, W., Tockstein, S., Moolani, H., Chavda, F., Badwaik, V., Lawrenz, M.B., Dakshinamurthy, R., 2016. Novel Synthesis of Kanamycin Conjugated Gold Nanoparticles with Potent Antibacterial Activity. *Frontiers in Microbiology*, Volume 7, p. 177773

Rosman, N.S.R., Masimen, M.A.A., Harun, N.A., Idris, I., Ismail, W.I.W., 2021. Biogenic Silver Nanoparticles (AgNPs) from Marphysa Moribidii Extract: Optimization of Synthesis Parameters. *International Journal of Technology*, Volume 12(3), pp. 635–648

Sani, A., Cao, C., Cui, D., 2021. Toxicity of Gold Nanoparticles (AuNPs): A Review. *Biochemistry and Biophysics Reports*, Volume 26, p. 100991

Sarhan, R.M., Kogikoski, S., Schürmann, R.M., Zhao, Y., Krause, A., Schmidt, B., Bald, I., Lu, Y., 2022. Colloidal Black Gold with Broadband Absorption for Photothermal Conversion and Plasmon-Assisted Crosslinking of Thiolated Diazonium Compound, ChemRxiv, Volume 2022, pp. 1–22

Shahriari, M., Hemmati, S., Zangeneh, A., Zangeneh, M.M., 2019. Biosynthesis of Gold Nanoparticles Using Allium Noeanum Reut. ex Regel Leaves Aqueous Extract; Characterization And Analysis of Their Cytotoxicity, Antioxidant, and Antibacterial Properties. *Applied Organometallic Chemistry*, Volume 33(11), p. 5189

Sofyan, N., Ridhova, A., Sianturi, M.C., Yuwono, A.H., 2019. Effect of NaCl Addition on Nano Rosette TiO2 Crystal Growth During Hydrothermal Deposition. *International Journal of Technology*, Volume 10(6), pp. 1235–1242

Song, J., Hwang, S., Park, S., Kim, T., Im, K., Hur, J., Nam, J., Kim, S., Park, N., 2016. DNA Templated Synthesis of Branched Gold Nanostructures with Highly Efficient Near-Infrared Photothermal Therapeutic Effects. *RSC Advances*, Volume 6(57), p. 51658–51661

Stanca, S.E., Fritzsche, W., Dellith, J., Froehlich, F., Undisz, A., Deckert, V., Krafft, C., Popp, J., 2015. Aqueous Black Colloids of Reticular Nanostructured Gold. *Scientific Reports*, Volume 5(1), p. 7899

Su, C., Huang, K., Li, H.H., Lu, Y.G., Zheng, D.L., 2020. Antibacterial Properties of Functionalized Gold Nanoparticles and Their Application in Oral Biology. *Journal of Nanomaterials*, Volume 2020, pp. 1–13

Tachibana, M., Yoshizawa, K., Ogawa, A., Fujimoto, H., Hoffmann, R., 2002. Sulfur-Gold Orbital Interactions Which Determine the Structure of Alkanethiolate/Au(111) Self-Assembled Monolayer Systems. *Journal of Physical Chemistry B*, Volume 106(49), pp. 12727–12736

Xue, Y., Li, X., Li, H., Zhang, W., 2014. Quantifying Thiol-Gold Interactions Towards the Efficient Strength Control. *Nature Communications*, Volume 5(1), pp. 1–9

Yu, R., Wang, J., Han, M., Zhang, M., Zeng, P., Dang, W., Liu, J., Yang, Z., Hu, J., Tian, Z., 2020. Overcurrent Electrodeposition of Fractal Plasmonic Black Gold with Broad-Band Absorption Properties for Excitation-Immune SERS. *ACS Omega*, Volume 5(14), pp. 8293–8298

Yulizar, Y., Utari, T., Ariyanta, H.A., Maulina, D., 2017. Green Method for Synthesis of Gold Nanoparticles Using Polyscias Scutellaria Leaf Extract under UV Light and Their Catalytic Activity to Reduce Methylene Blue. *Journal of Nanomaterials*, Volume 2017, p. 3079636

Zhang, Y., Shareena-Dasari, T.P., Deng, H., Yu, H., 2015. Antimicrobial Activity of Gold Nanoparticles and Ionic Gold. *Journal of Environmental Science and Health - Part C Environmental Carcinogenesis and Ecotoxicology Reviews*, Volume 33(3), pp. 286–327